Glass and Ceramics, Vol. 69, Nos. 9 – 10, January, 2013 (Russian Original, Nos. 9 – 10, September – October, 2012)

GLASS CERAMICS

UDC 666.263.2

SINTERING AND CRYSTALLIZATION DURING THE PRODUCTION OF STRONTIUM-ANORTITE GLASS CERAMIC

P. D. Sarkisov,[1] L. A. Orlova,[1, 3] N. V. Popovich,[1] R. Bruntsch,[1] A. S. Chainikova,[1, 4] K. Klinkmueller,[2] and N. E. Shchegoleva[1]

Translated from *Steklo i Keramika*, No. 9, pp. 28 – 36, September, 2012.

Crystallization and sintering, which occur during firing, during the production of strontium-anortite glass ceramics by means of powder metallurgy are studied. It is shown that the dispersity of the initial glass powder and the temperature–time firing regimes affect the crystallization temperature and heat, the nature of the precipitating phases and the sintering temperature interval and kinetics of the particles. It is determined that for ceramizing glass compositions there exists a narrow powder dispersity interval in which densely sintered materials with the required composition and high mechanical properties can be obtained using multistep heat-treatment.

Key words: glass ceramic, sintering, dispersity, strontium anortite, $SrO–Al_2O_3–SiO_2$.

In recent years interest in barium- and strontium-aluminum silicate glass ceramics has increased in Russia and abroad. A review of scientific-technical data and patents shows that glass ceramics of this type are promising for use as substrates for electronics, in the preparation of radioparent articles, and as matrices for high-temperature composite materials. A great deal of attention is being devoted to glass ceramics in the system $SrO–Al_2O_3–SiO_2$. This is because strontium-aluminum silicate glasses have high softening temperatures t_g (700 – 800°C) while the principal phase crystallizing in this system (monoclinic strontium anortite $SrAl_2Si_2O_8$) possesses together with low dielectric properties (ε and tan δ), a high melting point (1719°C), good mechanical properties (E = 100 GPa, σ_{bend} = 100 – 120 MPa) and quite low CLTE $(26 – 48) \times 10^{-7}$ K^{-1} [6].

Glass ceramic materials are successfully made using conventional glass methods and developing ceramic (powder) technologies. Powder technology makes it possible to use as the initial glass crystallizing glasses with an extremely wide range of compositions, including compositions that are unsuitable for use with the classical method — high-viscosity, "short" and with very low and very high crystallizability. In most cases the sintered materials acquire a uniform microcrystalline structure with a high content of a mineral phase. In addition, compared with the classical technology the physical-chemical properties of the material obtained are more stable and reproducible.

One of the most important stages in obtaining glass ceramic materials by powder technology is the sintering stage. The driving force of the sintering process is the excess surface energy of the particles. Sintering of glass powders is a liquid-phase process; it is described by the mechanism of viscous flow, and in general it is comprised of two stages. At the initial stage the particles of glass soften and converge on one another forming contacts in the process. This stage continues until the relative density of the green part is 80%; in the literature it is usually described by Frenkel's model, referring to an isothermal process and spherical particles of identical size. At the final stage a transition occurs from communicating to isolated pores in the material which subsequently becomes overrun. The removal of isolated pores starts at density 90%. The Mackenzie–Shuttleworth model describes this stage; this model is limited to the analysis of isothermal compaction of monodisperse glass powder [7].

The sintering of glass crystallizing during heat-treatment is a more complex process. In addition, compaction and crystallization can occur successively or concurrently. A cluster

[1] D. I. Mendeleev Russian Chemical-Technology University, Moscow, Russia.
[2] Mining Academy, Freiburg, Germany.
[3] E-mail: orlova@rctu.ru.
[4] E-mail: anna-chanikova@mail.ru.

model describing compaction and crystallization which occur in glass powders with a polydisperse distribution of irregularly shaped particles during nonisothermal heat-treatment is proposed in [8]. But even this model is far from reality. This is especially exacerbated by the fact that sintering and crystallization compete with one another. As a result, a separate investigation is required for each type of glass powder in order to determine the parameters of the initial powders and the firing conditions under which the material obtained sinters to the state with the highest possible density and crystallization occurs with the maximum precipitation of the crystalline phase determining the required working characteristics [9 – 13].

In 1980 – 1990, when sintered glass ceramics were first developed, the effect of many technological factors on sintering and crystallization of glass in aluminum-silicate systems (spodumene, cordierite, pyroxene) was studied and definite regularities were found, but many of the results were inconsistent and even contradictory [14 – 16].

In this connection the objective of the present work is to study in greater detail the effect of the main technological parameters — dispersity of the glass powder, rate of temperature rise, temperature-time parameters of heat-treatment — on the sintering and crystallization of glass with strontium-anortite composition using new-generation apparatus (DSC, laser particle-size analyzer, high-temperature dilatometer) as well as to develop well-grounded recommendations for choosing the parameters for obtaining a high-density sintered glass ceramic material with the required crystalline phase that secures the required working characteristics.

EXPERIMENTAL PROCEDURE

A glass composition which was used as a base to obtain radioparent glass ceramic containing the following (wt.%) was chosen for the experiments on the basis of previous work [17]: 20 SrO, 30 Al_2O_3, 40 SiO_2 and 10 TiO_2. Titanium dioxide was used as a crystallization catalyst and to lower the glass synthesis temperature. Despite the recommendations made by in [16] concerning the possibility of decreasing the concentration of the crystallization catalyst for obtaining glass ceramics by powder technology, in the present case 10% TiO_2 is the optimal quantitative addition for which the glassmaking temperature does not exceed 1580 – 1600°C.

The powders were obtained by grinding quenched glass. Strontium carbonate, alumina, quartz sand and rutile were used as the raw materials to prepare the batch. The glass was made in corundum crucibles at temperature 1600°C in an oxidative atmosphere followed by casting into water. The quenched glass was wet ground for 3 h in agate drums in a planetary mill. The powder obtained was separated on a vibratory screen, manufactured by the Netzsch company, into six fractions: 200 – 100, 100 – 70, 70 – 50, 50 – 20, 20 – 5 μm and < 5 μm.

The fraction compositions of the powders and their specific surface areas were determined by means of laser diffraction in Analysette 22 – NanoTec, MicroTec, Fritsch particle-size analyzers. The bulk density was calculated as the ratio of the mass of the powder freely poured into a measuring cylinder to filling.

The powders were pressed into 40 × 6 × 5 mm rods. A 5% solution of polyvinyl alcohol was used as a temporary process binder. The pressing pressure was 100 MPa. To study the crystallization process in detail the materials were fired at 900, 1000, 1100 and 1350°C for 30 min with temperature rise rate 5 K/min.

A STA 449 C Jupiter – Netzsch thermal analyzer was used to study the physical-chemical processes occurring when glass powders are heated in the interval 20 – 1550°C. The crystallographic phases were determined by x-ray phase analysis (XPA) using a DRON-3M diffractometer; the identification was made on the basis of the JCDFS electronic catalog of diffraction patterns (Joint Committee on Powder Diffraction Standards). A DIL 402 PC – Netzsch high-temperature horizontal dilatometer was used to study sintering, the criterion for which is the amount of shrinkage. The measurements were performed on samples in the form of small rods at least 20 mm long. To compare the DSC and dilatometry data, which contain information on crystallization and sintering of powders with different particle size, the same rate of heating 5 K/min was used.

The hydrostatic weighing method was used to measure the porosity, density and water absorption of the fired samples. A microprobe complex based on a Jeol JSM–6480LV scanning electron microscope was used to analyze the microstructure of the materials. The professional, licensed SEM Control User Interface software was used to process the results.

EXPERIMENTAL RESULTS

The data from laser dispersion analysis of the experimental fractions are presented in Fig. 1. It follows that the particle shape is far from spherical and as the particle size decreases, the dispersity of the powders increases. The results characterizing the dominant particle size, the specific surface area and the bulk density of the initial powders are presented in Table 1. It is evident that as particle size decreases the bulk density of the powders decreases. This is because powder adsorption capacity increases as the specific surface area of the particles increases.

The DSC study of the physical-chemical processes occurring during heating of the glass powders (Fig. 2) showed that the vitrification temperature t_g of large glass particles lies in the interval 750 – 780°C; it is impossible to determine t_g for particles smaller than 38 μm. The exothermal effects at temperatures 940 – 950 and 1050 – 1080°C correspond to the precipitation of tialit Al_2TiO_5 and monoclinic strontium anortite $SrAl_2Si_2O_8$ phases, respectively. The endo effects in

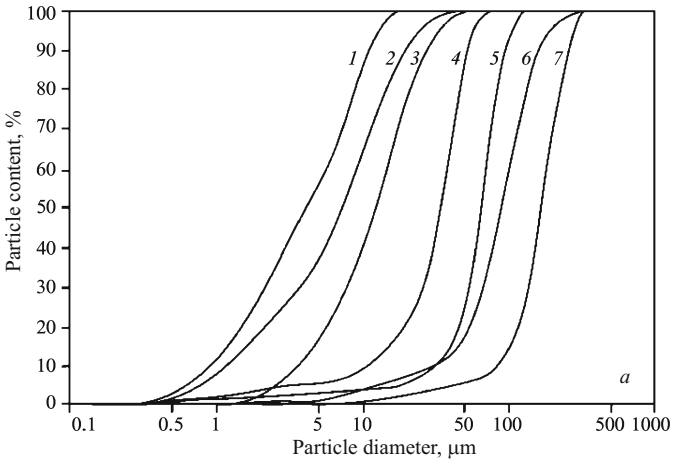

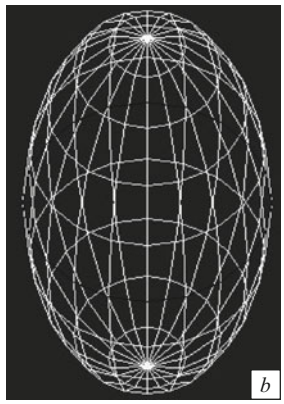

Fig. 1. The results of a dispersion analysis of the experimental fractions of glass powders: *a*) integral particle-size distribution curves: *1*) < 5 μm; *2*) 5 – 10 μm; *3*) 10 – 20 μm; *4*) 20 – 50 μm; *5*) 50 – 70 μm; *6*) 70 – 10 μm; *7*) 100 – 200 μm; *b*) model of 4 μm powder particles, length-to-diameter ratio 2 : 3.

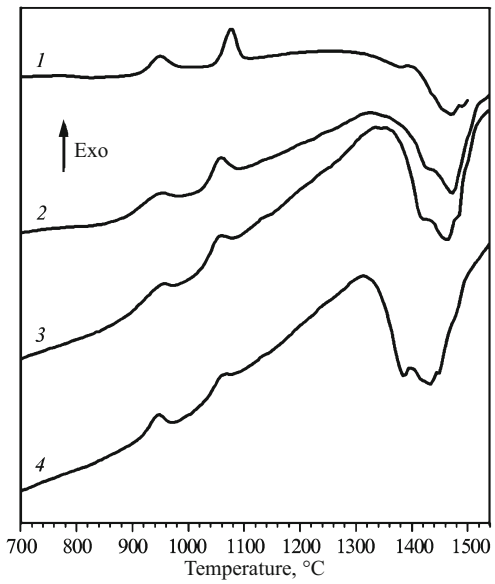

Fig. 2. DSC curves for glass powders with predominant particle size: *1*) 164, *2*) 38, *3*) 10 and *4*) 4 μm.

the temperature range 1310 – 1500°C correspond to softening of the residual glass phase and successive dissolution of the precipitated crystalline phases in it. As the dispersity of the powders increases all temperatures shift to lower values. X-ray Phase Analysis confirms these date (Fig. 3). After soaking at 900°C the samples obtained from powders with particles larger than 89 μm are amorphous, while for smaller powder particles crystallization has already started (Fig. 3*a*) and is all the more active the greater the dispersity of the powder. As the temperature increases the effect of dispersity on the phase composition of the material virtually vanishes and crystallization is intense in all samples (Fig. 3*b*). The main crystalline phases are monoclinic strontium anortite and tialit. It follows that as the particles become smaller crystallization at the initial stage becomes more intense. This is effect is strongest for powders with particles smaller than 4 μm.

Analysis of the DSC curves showed that as the powder dispersity increases the exothermal peaks corresponding to precipitation of tialit and monoclinic anortite broaden, and the formation heats of phases change (Fig. 4).

Curves of shrinkage in the temperature interval 20 – 1500°C (Fig. 5) were obtained for all experimental fractions of glass powders and the compaction rates (first derivative of the shrinkage) at different stages of sintering (Fig. 6) were determined.

Comparing the DSC data, dilatometric shrinkage curves (see Fig. 5) and curves of the shrinkage rate of change in the course of heating (see Fig. 6) shows that the samples start to sinter above the vitrification temperature t_g in the temperature range 840 – 860°C. The entire sintering interval can be divided into three stages:

stage I) sintering before the first crystalline phase (tialit) precipitates;

stage II) sintering accompanied by simultaneous crystallization of tialit and continuing compaction; this stage is completed at the moment anortite crystallization starts;

stage III) completing sintering, occurring after crystallization and determined by the softening temperature of the residual glass phase.

The experimental fraction interval can be conventionally divided into three groups according to the nature of the effect of powder dispersity on the amount and rate change (Figs. 7 and 8) of the shrinkage of the samples:

TABLE 1. Powder characteristics

Powder fraction, μm	Dominant particle size, μm	Specific surface area, 10^3 m^2/kg	Bulk density, g/cm^3
200 – 100	164	0.0646	1.54
100 – 70	89	0.1060	1.36
70 – 50	64	0.2610	1.26
50 – 20	38	0.5607	1.18
20 – 10	18	0.6260	0.82
10 – 5	10	1.8490	0.78
< 5	4	3.1158	0.70

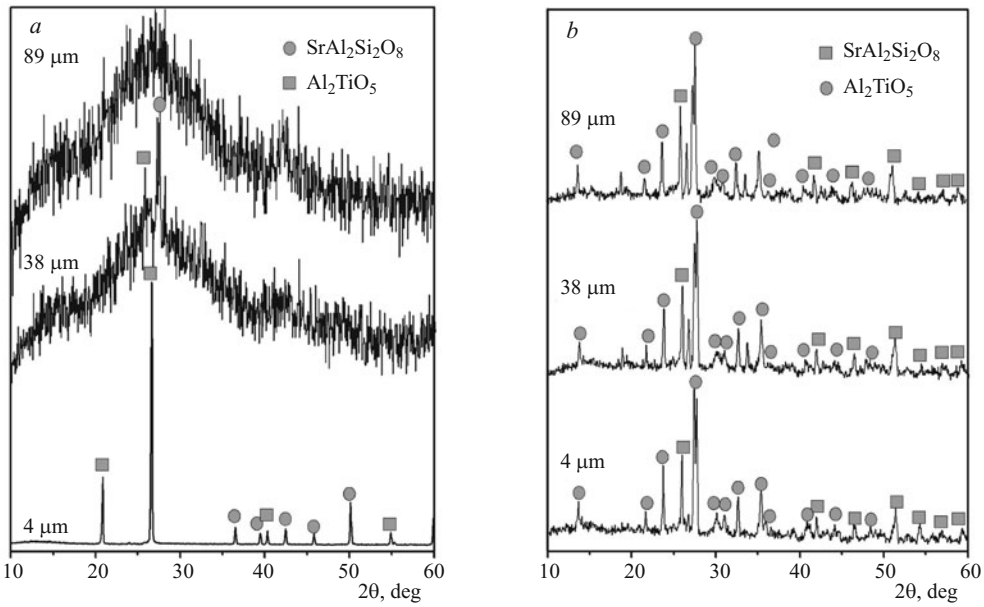

Fig. 3. X-ray diffraction patterns of samples having different dispersity and heat-treated at 900°C (*a*) and 1350°C (*b*).

– large fraction – from 200 to 70 μm; for this fraction the shrinkage occurs during the first stage of sintering at temperatures below the onset of tialit precipitation according to a purely viscous mechanism and is 7 – 8.5%; the shrinkage rate is 32.4 – 33.6 %/h;

– medium fraction – from 70 to 20 μm; shrinkage is intense in a wide temperature interval at the sintering stages I and II below the precipitation temperature of the second crystalline phase Sr-anortite and is 14 – 15%, reaching a maximum for powders with the predominant particle size 38 μm; for this powder a maximum of the compaction rate is observed in both stages; it should be noted that even though a crystalline phase precipitates (tialit), the compaction rate at the stages I and II changes very little, which could attest to a very small increase of the apparent viscosity of the system owing to the crystallization of tialit;

– for the fine fraction (< 20 μm) intensification of crystallization characteristic and leads to an increase of the viscosity of the system and impedes sintering; as a result the shrinkage rate and amount at the first two stages decrease considerably; sintering is most complete at the final stage after the glass is completely crystallized.

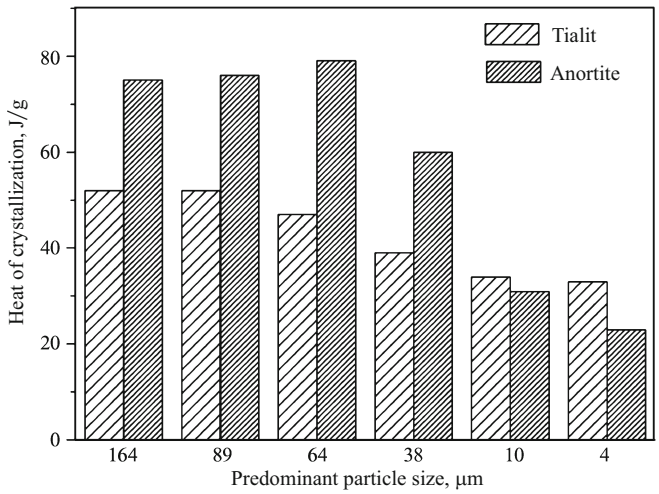

Fig. 4. Heat of crystallization of tialit and strontium anortite versus powder dispersity.

DISCUSSION

Analysis of the data confirms that the dispersity of the particles when using powder technology is together with the chemical composition and structure of the glass the most important factor influencing the process of obtaining a completely sintered glass ceramic with the required phase composition [7, 13].

The competition between the compaction or crystallization processes is determined by the particle size and, correspondingly, the amount of free energy accumulated by the powders during comminution and driving the sintering process as well as by the surface area of the glass-powder particles and their defect density, which determine crystal nucleation and growth.

The authors of a number of works [6, 18] indicate that the proclivity of glasses to sinter is characterized by the magnitude of the interval between the vitrification and crystallization onset temperatures $t_g - t_{cr}$. The experimental data obtained in the present work show that the sintering onset temperature t_{sin} for large particles of glass powder (200 – 70 μm) lies about 100°C above t_g. For smaller particles, as indicated above, t_g cannot be determined from the DSC data because there is no endo effect preceding the first exo peak, probably because of the heightened crystallizability of fine glass powders. The limitation of the sintering interval by the crystallization temperature must also be determined more accurately. The results obtained show that it is only for large particles

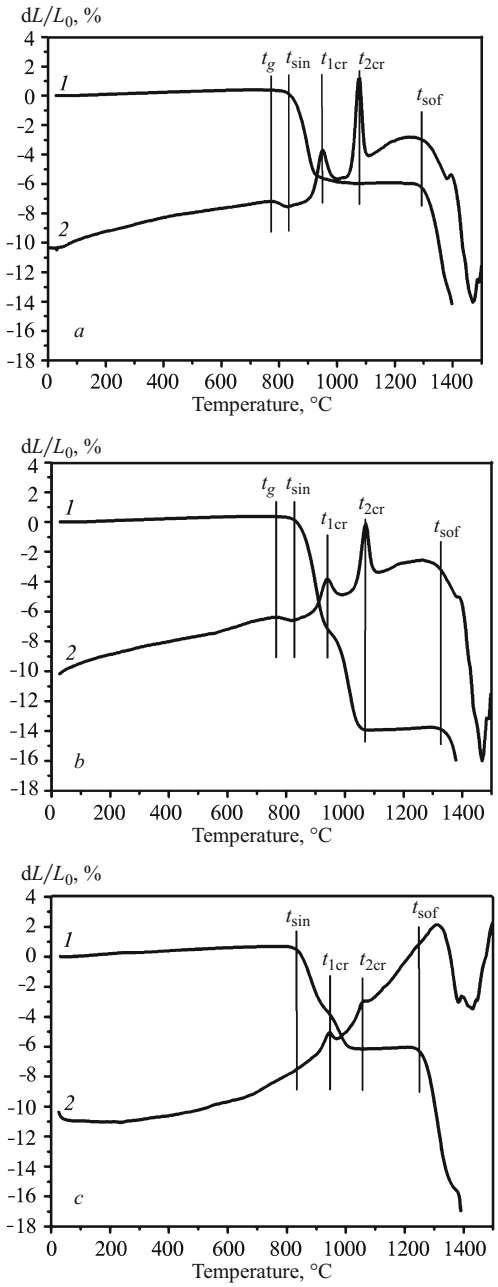

Fig. 5. Curves of linear shrinkage during heat (*1*) and DSC (*2*) for samples with the dispersity of the initial powders: *a*) 164, *b*) 64 and *c*) 4 μm; t_g , t_{sin} , t_{1cr} , t_{2cr} , t_{sof}) vitrification, sintering onset, crystallization temperatures of tialit, anortite and softening temperature of the residual glass phase, respectively.

(200 – 70 μm) that sintering stops with the onset of crystallization (see Fig. 5*a*). As the fineness of the grinding increases it becomes possible for sintering and precipitation of a crystalline phase (tialit) to occur concurrently, and it is only with the onset of precipitation of the main silicate phase (Sr-anortite) that sintering ceases. It follows that the sintering interval of the crystallizing glasses should be determined empirically according to the shrinkage curves taking account of the rate of heating.

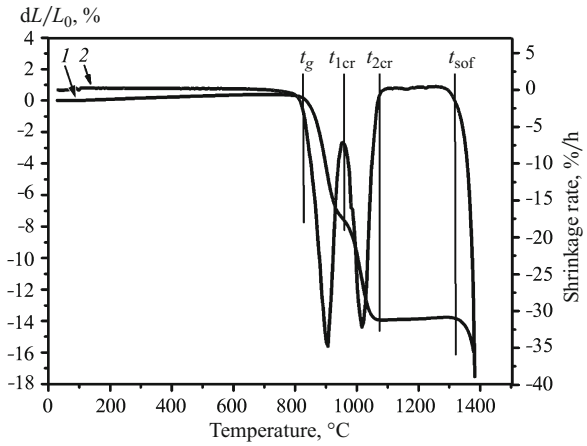

Fig. 6. Curves of the linear shrinkage *1* and change of shrinkage rate (first derivative) during heating *2* for a sample with dispersity 64 μm; see Fig. 5 for abbreviation conventions.

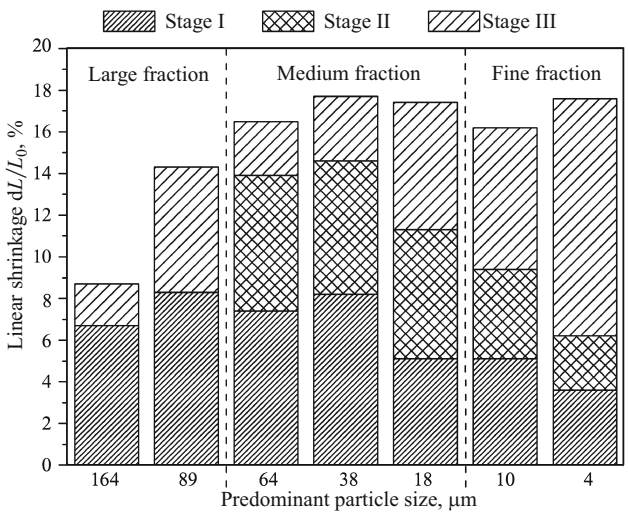

Fig. 7. Shrinkage amount for samples at different sintering stages versus the dispersity of the initial powders.

The dependence of the sintering interval determined from dilatometric curves (see Fig. 5) on the particle dispersity is presented in Fig. 9 for the glass powders studied in the present work. For the large particle fraction of powders with average particle size to 89 μm this interval corresponds to stage I sintering and it is very narrow, of the order of 65°C wide. The degree of sintering reached in this interval is low and the removal of residual pores becomes possible only at stage III as a result of softening of the residual glass phase.

Increasing the powder dispersity to 38 μm makes it possible to increase the width of the sintering interval to 180°C as a result of the appearance of stage II at which, as indicated above, sintering proceeds simultaneously with the precipitation of the first crystalline phase; the total shrinkage increases to 14.5% (see Fig. 7) and the process proceeds at the maximum rate (see Fig. 8). However, just as for large parti-

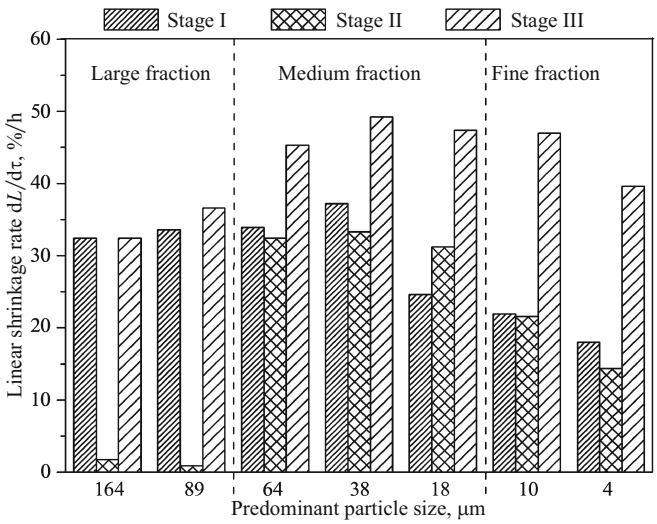

Fig. 8. Rate of linear shrinkage of the samples at different sintering stages versus the dispersity of the initial powders.

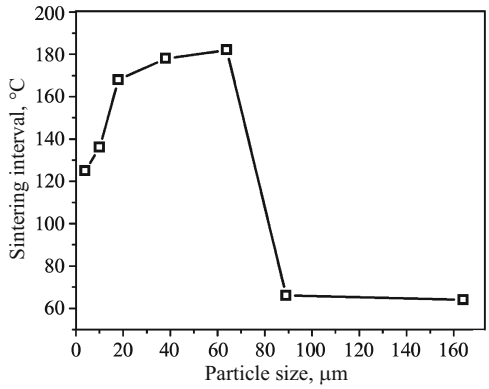

Fig. 9. Width of the sintering interval versus the dispersity of glass powders.

cles soaking at stage III is necessary in order to maximize compaction.

For even smaller glass-powder particles (to < 18 μm) the sintering interval decreases to 120°C and at the same time the shrinkage decreases (to 6%) as does the compaction rate (see Fig. 8). The greatest shrinkage occurs mainly at stage III near the softening temperature of the residual glass phase.

The explanation of these results is as follows. Glass powders sinter according to the viscous flow mechanism and the sintering is determined by the surface tension, particle size and viscosity of the system. For large particles the dominant factor affecting sintering is particle size, with respect to which shrinkage is in inverse proportion. For smaller particles (< 70 μm) the effect of this factor decreases; but, most importantly, for 70 – 20 μm particles, sintering continues even though tialit precipitates in the temperature interval 900 – 950°C. This is probably because, as approximate calculations show, the amount of this phase does not exceed 15% and its precipitation does not greatly affect the composition of the residual glass phase, which remains enriched with the alkaline-earth oxide SrO. In this connection the viscosity of the system does not change much, and sintering can continue in parallel with crystallization.

For glass powders with particles of such sizes crystallization is mainly of a volume character, as is typical for monolithic glass, in which the crystallization catalyst(titanium dioxide) plays the leading role, which consists of liquation of glass with formation of two glass phases: aluminum titanate and strontium-aluminum silicate with precipitation of the primary crystalline phase tialit and, as temperature increases, monoclinic strontium anortite.

For still smaller particles (< 20 μm) the crystallization process competing with compaction shifts to lower temperatures. This is determined by the fact that for a given particle size (< 10 μm) surface crystallization of glass due to the extended surface and excess surface energy, which the particles acquire during comminution, prevails. As a result the temperature interval of sintering stages I and II contracts, which sharply decreases the degree of compaction attainable at these stages. The fact that the crystallization temperature decreases on account of the surface component is indicated by the absence of t_g on the DSC curves (see Fig. 2) of fine glass powders; the broadening of the exothermal peaks in these curves shows that surface crystallization makes the predominant contribution to the total crystallization. The possibility of such an interpretation of the broadening of exo peaks is also indicated in [10]. The fact that the decrease of the formation heat of crystalline phases (see Fig. 4) with increasing dispersity also gets our attention. Because of their active crystallization (volume and surface) fine glass powders sinter mainly at stage III as a result of the viscous flow of the residual glass phase. At this stage of sintering shrinkage comprises 12% for powders with 4 μm particles predominating but no more than 2% for larger particles.

It should also be noted that the size of the initial glass particles also affects the structure of the glass ceramic material. As the powder particles decrease in size the structure of the fired material becomes more fine-crystalline (Fig. 10).

The results show that for ceramizing glass compositions the particle size becomes determining in the synthesis of sintered glass ceramics on the basis of such compositions, and the particle-size dependence of the compaction is extremal. This means that if grinding fineness must be minimized during ceramic production or sintering of non-crystallizing glass in order to intensify the compaction process, then in obtaining sintered glass ceramic based on ceramizing glass compositions there exists a near interval of dispersity where the sintering process at the initial stage prevails over crystallization and subsequently can proceed concurrently with precipitation of a crystalline phase, but this depends on its composition and amount.

The present work has established that in non-isothermal sintering of strontium-anortite glass powders with titanium dioxide as the crystallization catalyst maximum compaction

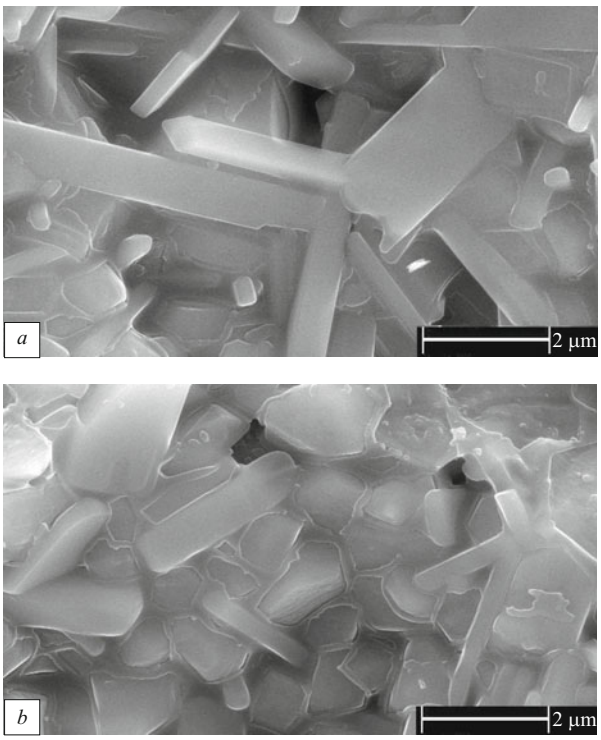

Fig. 10. Electron microscope images of samples with initial-powder dispersity 64 μm (*a*) and 4 μm (*b*), fired at 1350°C.

is reached for powders with dispersity 20 – 50 μm and dominant particle size 38 μm. Heat-treatment is best done in four steps: the temperatures at the first two and last steps must correspond to the temperatures of the maximum shrinkage rate at these three stages; prior to the last stage of isothermal soaking there must be a temperature stage that corresponds to the maximum rate of precipitation of the dominant silicate phase that determines the working characteristics of the sintered glass ceramic.

Following the recommendations made here, for the strontium-aluminum-silicate glass powder studied with optimal dispersity 20 – 50 μm heat-treatment was conducted with soakings at 900, 1020, 1180 and 1350°C with heating rate 5 K/min. The indicators of the material obtained were better than those of previously sintered materials [17]; the material was characterized by open porosity 0.3%, relative density 96%, bending strength 130 MPa and microhardness 9600 MPa.

CONCLUSIONS

In summary, it has been shown here that the particle size of initial glass powders strongly affects the sintering process and the amount, rate and temperature interval of shrinkage. For ceramizing glass compositions there exists a narrow interval of dispersity for the powders which can be used to obtain densely sintered materials with the required phase composition and high mechanical properties using a multistep heat-treatment regime.

REFERENCES

1. G. H. Beall, “Refractory glass-ceramics based on alkaline earth aluminosilicates.” *J. Euro. Ceram. Soc.*, No. 29, 1211 – 1219 (2009).
2. *Refractory Glass Ceramics. US Patent 2009/0056380Al, No. 11/895847*; filed August 28, 2007; published March 5, 2009.
3. N. P. Bansal, “Fiber-reinforced strontium aluminosilicate glass-ceramic composites,” *J. Mater. Res.*, **3**(12), 745 – 753 (1997).
4. F. Ye, L. Liu, Y. Wang, Y., Zhou Y et al., “Preparation and mechanical properties of carbon nanotube reinforced barium aluminosilicate glass–ceramic composites,” *Scr. Mater.*, No. 55, 911 – 914 (2006).
5. L. Liu, F. Ye, Y. Zhou and Z. Zhang, “Microstructure compatibility and its effect on the mechanical properties of the α-SiC/β-Si_3N_4 co-reinforced barium aluminosilicate glass ceramic matrix composites,” *Scr. Mater.*, No. 63, 166 – 169 (2010).
6. Y. M. Sung and S. Kim, “Sintering and crystallization of off-stoichiometric $SrO \cdot Al_2O_3 \cdot 2SiO_2$ glasses,” *J. Mater. Sci.*, No. 35, 4293 – 4299 (2000).
7. M. O. Prado and E. D. Zanotto, “Glass sintering with concurrent crystallization,” *C. R. Chimie*, No. 5, 773 – 786 (2002).
8. M. O. Prado, E. D. Zanotto, and R. Muller, Model for sintering polydispersed glass particles,” *J. Non-Cryst. Solids*, No. 279, 169 – 178 (2001).
9. R. Huang, J. Pan, A. R. Boccaccini and Q. Z. Chen, “A two-scale model for simultaneous sintering and crystallization of glass-ceramic scaffolds for tissue engineering,” *Acta Biomater.*, No. 4, 1095 – 1103 (2008).
10. K. Lambrinou, O. Biest, A. R. Boccaccini and D. M. R. Taplin, “Densification and crystallization behavior of barium magnesium aluminosilicate glass powder compacts,” *J. Euro. Cer. Soc.*, No. 16, 1237 – 1244 (1996).
11. A. R. Boccaccini, W. Stumpfe, D. M. R. Taplin and C. B. Ponton, “Densification and crystallization of glass powder compacts during constant heating rate sintering,” *Mater. Sci. Eng.*, **A219**, 26 – 31 (1996).
12. L. Lefebvre, L. Gremillard, J. Chevalier, et al., “Sintering behavior of 45S5 bioactive glass,” *Acta Biomater.*, No. 4, 1894 – 1903 (2008).
13. M. Mohammadi, P. Alizadeh and Z. Atlasbaf, “Effect of frit size on sintering, crystallization and electrical properties of wollastonite glass-ceramics,” *J. Non-Cryst. Solids*, No. 357, 150 – 156 (2011).
14. V. N. Filipovich, A. M. Kalinina and D. D. Dmitriev, “Surface nucleation of crystals of volume crystallization of glass in power technology of glass ceramics,” in: *Catalyzed Crystallization of Glass* [in Russian], GIS, Moscow (1986), pp. 29 – 34.
15. V. N. Sigaev, P. D. Sarkisov, T. É. Aslanyan, et al., “Effect of technological factors on the crystallization of cordierite glass,” *Fiz. Khim. Stekla*, **20**(6), 772 – 778 (1994).
16. V. I. Solov’ev, “Role of crystallization catalysts in powder technology of glass ceramics,” in: *Catalyzed Crystallization of Glass* [in Russian], GIS, Moscow (1986), pp. 111 – 114.
17. *Radioparent Glass Crystalline Material for Aviation Engineering, RF Patent 2440936, No. 2010145410/03* [in Russian], application November 9, 2010; published January 27, 2012.
18. A. Marotta, A. Buri and F. Branda, “Heterogeneous bulk nucleation and differential thermal analysis,” *J. Thermal Anal.*, **21**, 227 – 233 (1981).